

In-Pavement Wireless Sensor Network for Vehicle Classification

Ravneet Bajwa, Ram Rajagopal, Pravin Varaiya and Robert Kavalier

Sensys Networks, Inc
2560 Ninth Street, Suite 219
Berkeley CA 94710

{rbajwa, rrajagopal, pvaraiya, kavalier}@sensysnetworks.com

ABSTRACT

Vehicle classification data, especially for trucks, is of considerable use to agencies involved in almost all aspects of transportation and pavement engineering. Current technologies for classification involve expensive installation and calibration procedures. A wireless sensor network (WSN) for vehicle classification based on axle count and spacing was designed, calibrated, tested, and deployed near a weigh station in Sunol, California. The WSN includes: vibration sensors which report pavement acceleration; vehicle detection sensors which report vehicle's time of arrival and departure; and an Access Point (AP) that logs the data collected from all these sensors. Both sensors are packaged for durability, occupy minimal space, have long lifetimes, and are embedded inside the pavement. The vibration sensors are capable of over-the-air software programming and are designed to be immune to sound. Vibration and classification ground truth data for 53 different trucks exiting the weigh station were collected. The vibration data collected at 512 Hz had an accuracy of 400 μg . A novel algorithm for estimating axle count and spacing has been developed. The combination of bandwidth-aware smoothing filter and peak detector that we use in this algorithm could be useful in many other applications. The algorithm successfully classified all 53 trucks.

Categories and Subject Descriptors

C.3 [Special-Purpose and Application-Based Systems]: Realtime and Embedded Systems, Signal Processing Systems; I.5.4 [Applications]: Signal Processing, Waveform Analysis

General Terms

Design, Experimentation, Algorithms

Keywords

Sensor Networks, Vehicle Classification, Energy Detector,

Permission to make digital or hard copies of all or part of this work for personal or classroom use is granted without fee provided that copies are not made or distributed for profit or commercial advantage and that copies bear this notice and the full citation on the first page. To copy otherwise, to republish, to post on servers or to redistribute to lists, requires prior specific permission and/or a fee.

IPSN'11, April 12–14, 2011, Chicago, Illinois.

Copyright 2011 ACM 978-1-4503-0512-9/11/04 ...\$10.00.

Axle Detection, Traffic Monitoring

1. INTRODUCTION

Transportation agencies collect vehicle classification information to plan highway maintenance programs, evaluate highway usage and optimize the deployment of various resources on the road. Vehicles are typically classified into different categories, such as passenger vehicles, buses and trucks of different sizes. There are many classification schemes but the most common ones use axle counts and the spacing between axles to assign vehicles to different classes [7].

Currently, various technologies are used for classification. Existing intrusive technologies such as piezoelectric sensors and inductive loops have very high installation and maintenance costs and non-intrusive technologies such as infrared and video imaging are sensitive to traffic and weather conditions [18]. In this paper we propose an alternative system based on a Wireless Sensor Network (WSN) that is both cost effective and insensitive to environmental conditions.

The solution is based on a carefully designed sensor system that is deployed in the pavement and is capable of measuring the vibrations of the road caused by a moving vehicle and the speed of a vehicle traveling on the road. A novel event detection algorithm that combines measurements of multiple sensors is used to provide an axle count and the spacing between axles for each vehicle. The sensor system can be installed on a road in less than 20 minutes [23]. Vehicles can travel at normal speeds and no special lane is required. There are many difficult challenges in this concept: the road environment is very noisy, there are severe power constraints and the correspondence between vehicle axles and pavement vibration is not well understood. In this paper we detail how each one of these challenges were addressed by our system design. To the best of our knowledge, this is the first in-pavement, easy to deploy, WSN based system for counting axles and determining axle spacing for vehicles traveling in a traffic lane.

2. WSN SYSTEM FOR CLASSIFICATION

In this section we state the problem of vehicle classification, propose a wireless sensor network system for the problem and detail the main challenges that need to be addressed. We conclude by reviewing the related literature.

2.1 Problem statement

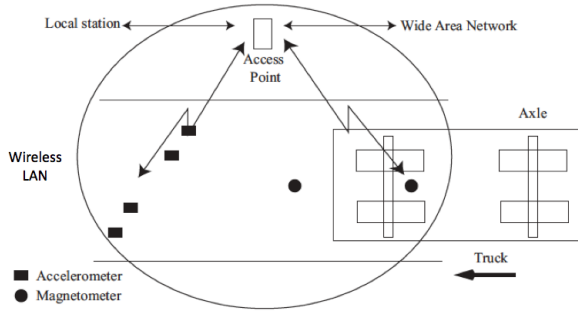


Figure 1: Wireless Sensor Network for vehicle classification: four accelerometer sensors and two magnetometer sensors. Truck moving from right to left is detected, its speed measured, and individual axles counted and measured.

The problem of vehicle classification consists of classifying vehicles traveling in a traffic lane into one of several classes. Examples of typical classes are: cars, buses, three-axle single unit trucks, and five-axle single trailer trucks. The national standard for vehicle classification in the US is given by the Federal Highway Administration (FHWA) [7]. One of the most widely implemented schemes for automatic vehicle classification is *scheme F* [13]. It uses the number of axles (*axle count*) and the distance between each axle (*axle spacing*) to assign vehicles into the different classes. The performance of the procedure relies on the accuracy of measuring these two quantities.

The classification problem can be stated as: *a vehicle travels in a traffic lane at some varying speed and we wish to count the number of axles and the spacing between each axle in an accurate manner.*

There are important challenges that need to be addressed by any solution to this problem. First, any proposed system should be able to count vehicle classes in individual lanes. This already poses a significant difficulty for side of the road solutions or even cameras, which require existence of overpasses or installation of gantries. Moreover, the solution should be sturdy and reliable enough to last many years to avoid disruptive and expensive lane closures. The measurements need to be accurate independent of time of day and weather conditions. The system should work in the noisy highway environment. It should be able to account for vehicle wander i.e. vehicles may move slightly off-center in a given lane. The wander is especially important when systems are installed at the exit of inspection facilities on the highway.

Finally, installation and operation costs should be kept at a minimum to enable wide deployment. The most substantial cost components are the loss of productivity associated with lane closures, extensive pavement repairs and gantry installation requirements. These costs are easily five to ten times more than the cost of the measurement system. For the same reason, the operation cost is directly related to the lifetime of the system, since maintenance usually requires at least a lane closure.

2.2 Proposed WSN System

One approach to reduce installation costs is to use the

highway pavement itself as a transducer¹. As an axle moves on the top of the road pavement it excites the structure locally and causes it to vibrate. These vibrations could be measured by a vibration sensor (accelerometer) embedded in the road. The important question is whether the vibrations induced by individual axles of a vehicle can be separated. The hope is that since the road pavement is not very elastic, vibrations are well localized in time and space. A commonly accepted model of this system is a moving impulse on an elastic beam [21]. The acceleration response at a fixed location is then a decaying signal that peaks when the vehicle reaches that location. A more detailed description of this fact is given in Appendix A.

We propose a sensor network system based on this concept. The sensor network comprises of three main components (Figure 1): vehicle detection sensors, vibration sensors, and an Access Point (AP). The vehicle detection sensors, based on magnetometers, report the arrival and departure times of a vehicle. The velocity of a vehicle is calculated by using two such sensors and their known spacing. The vibration sensors measure and report the acceleration of the pavement when a vehicle passes by. This data is used to detect/count individual axles of a vehicle and to calculate the axle spacings. The AP serves as the central entity of the network. It is used to send different commands to the sensors and to log the incoming data from all sensors.

There are three main challenges to create a system that works in practice: measuring the vehicle speed accurately, measuring the road vibrations accurately, and detecting and timing individual vehicle axles from these measurements. We explain each of the challenges in more detail.

2.2.1 Wireless vehicle detection sensor

The vehicle detection system measures the changes in magnetic field to infer the local presence of a vehicle. This along with the AP are available as a Vehicle Detection System for traffic monitoring [11]. Each sensor reports a time of arrival t_a and time of departure t_d of the vehicle as it arrives at the sensor and traverses it.

The sensors are easy to install (see Section 5.2), have low maintenance cost and very good performance. Multiple sensors installed in different lanes cooperatively transmit information using Synchronous Nanopower Protocol (SNP), a TDMA based protocol that schedules sensor transmissions to reduce power consumption. The proposed design lasts 10 years with a single 7200 mAhr battery. A typical sensor node is shown in Figure 2.

Vehicle speed and length. A pair of sensors (i, j) installed at a fixed known distance ($d_{ij} = 20'$) apart from each other are used to estimate speed accurately. Given the arrival times t_{ai} and t_{aj} at the two sensors i and j , the speed v is given by $v = \frac{d_{ij}}{|t_{aj} - t_{ai}|}$. A similar estimate can be obtained by using the departure times. The speed can be used to estimate the length (L) of the vehicle as $L = v(t_{dj} - t_{dj})$. These measurements have been shown to be very accurate in practice [11].

2.2.2 Wireless vibration sensor

The wireless vibration sensor consists of an accelerometer whose analog output is sampled and transmitted via a ra-

¹Installation of a small sensor is much cheaper and convenient than installing special material pavements required for piezoelectric sensors and load cells.

dio. Designing a sensor that measures pavement vibrations for axle detection has many unique challenges: the installed sensor’s noise has to be much smaller than the pavement acceleration resulting from even the lightest vehicle; the sensor has to be well coupled to the roadway and be resistant to heavy vehicle traffic; the sensor needs to sample fast enough to capture the transient vibrations in the pavement; the vibrations due to truck engines and other sounds should have a minimal effect on sensor readings; the sensor needs to be insensitive to the vehicles traveling in the neighboring lanes and should have a long lifetime.

The sensor resolution target of $500 \mu\text{g}$ and bandwidth of 50Hz is chosen based on field measurements and simulations reported in [1, 21]. The sampling frequency is chosen to be 5 times greater than the Nyquist Frequency [20], so we target 512 Hz. The constraint in this case is power consumption increase for higher sampling rates. We address the other challenges in detail in the upcoming sections.

2.2.3 Axle detection and counting

Given vehicle speed measurement and a reliable measurement from the wireless vibration sensor, we still need to construct an axle detection algorithm that has good performance. There are two important challenges in detecting individual axles: the vibration signals from successive axles tend to blend and in wide highway lanes, vehicles can experience significant wander. In this paper we introduce an approach that can handle both challenges by relying on a nonlinear event detection technique. The proposed technique can be useful in other problems as well.

2.3 Related Work

We identify three areas related to this work: applications of wireless sensor networks (WSN) to transportation, applications of vibration sensor networks in infrastructure monitoring and systems for vehicle classification.

Applications of WSN in transportation have been growing. For example, WSNs have been used for vehicle detection using magnetic sensors [4, 15, 23] and increasing road safety by intervehicular information sharing [22]. Much less has been done in terms of monitoring the response of road infrastructure itself.

Monitoring large infrastructures using accelerometer sensor networks has been studied for structural monitoring of bridges [14, 26], buildings [3] and underground structures such as caves [16]. In these particular cases, the sensor did not require embedding in the structure itself, although some of the applications could clearly benefit from the reduced noise and increased sensitivity in measurements. Wired embedded sensors in concrete structures have been investigated [17] but usually require complex installation procedures and have limited lifetime if used in roads.

Systems for vehicle classification can be divided into intrusive and non-intrusive schemes[7]. Most common non-intrusive schemes are based on digital imaging [10], range sensors[12], acoustic[19], infrared and microradar sensors. These systems suffer from accuracy issues with varying daylight, weather, and traffic conditions; have special requirements for setup; and multiple systems are required for high accuracy. More importantly, they may require special arrangements for measuring multiple lanes at sites without an overpass. The most common intrusive schemes are based on either piezoelectric sensors or magnetic loop detectors.

Piezoelectric sensors are used to estimate axle count and spacing. Loop detectors provide electric signatures proportional to vehicles that traverse the loop, and the data can be used for classification [25]. Both systems are costly to install and also costly to maintain.

More closely related to this paper, a vehicle classification scheme based on vehicle length and magnetic signature classification [4] has been proposed and evaluated, but it is shown to be very data intensive. A WSN system for vehicle detection and classification was proposed [6] combining acoustic, infrared and seismic. Its main application is for classification of vehicles in open fields, and its performance is dependent on environmental and other conditions. The main limitations seem to be cost and the difficulty for separating classification for different lanes.

3. IN-PAVEMENT WIRELESS VIBRATION SENSOR

This section develops and implements the sensor design for the wireless vibration sensor, including the choice of accelerometer, casing and noise mitigating filters. We then describe in detail the communication protocol developed for this sensor node. We continue by explaining the calibration procedure required for accurate readings. We conclude by benchmarking the performance of the sensor in some controlled experiments to verify digitization performance and power consumption.

3.1 Sensor Design

3.1.1 Resolution: selecting an accelerometer

	SD1221-005	MS9002.D
Sensitivity (V/g) @ 5V	2	1
Noise Density ($\mu\text{g}/\sqrt{\text{Hz}}$)	5	18
Current Consumption (mA)	8	≤ 0.4
Min. Operating Voltage (V)	4.75	2.5

Table 1: Comparison of important properties of accelerometers.

To build a sensor with $500\mu\text{g}$ sensitivity and 50 Hz bandwidth, we evaluated two different MEMS accelerometers: SD1221-005 from Silicon Designs and MS9002.D from Colibrys [5, 24]. These were selected from amongst many others in the market because of their very low noise density ($\mu\text{g}/\sqrt{\text{Hz}}$) and high sensitivity (V/g). As seen in Table 1, SD1221-005 has higher sensitivity and lower noise density than MS9002.D, both of which are very desirable characteristics. However, SD1221-005 consumes more than 20 times the current consumed by MS9002.D and has to be operated at a much higher voltage. Consistent with the table, SD1221-005 outperformed MS9002.D during our evaluation of the devices but both devices achieved our aimed minimum resolution of $500 \mu\text{g}$. We selected MS9002.D due its low operating voltage and low current consumption.

3.1.2 Noise: filters for mitigating sound noise

One of the problems that is often underreported about systems using accelerometers is their sensitivity to sound. A sensitive accelerometer such as the MS9002.D behaves like a microphone under the device’s bandwidth. A single

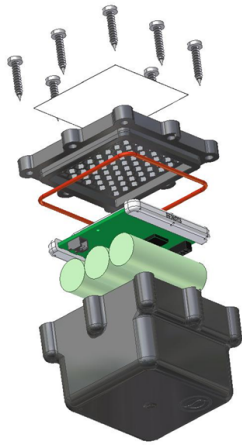


Figure 2: Packaging of the sensors in a sealed case.

pole anti-aliasing filter is not sufficiently aggressive to attenuate the interference due to sound under 1 kHz. A simple clapping sound near the accelerometer is picked up by the sensor as vibration. Thus, any sensor deployed in the open is vulnerable to this interference. It is reported in [1] that a 3rd order (or higher) low-pass filter with cutoff frequency of 50 Hz is sufficiently aggressive to filter out most of the sound in the audible spectrum. We use a 3rd butterworth filter with transfer function

$$H(j\omega) = \frac{1}{(1 + \frac{j\omega}{50})^2(1 + \frac{j\omega}{500})}$$

The filter is less aggressive for the frequencies of interest ($< 50\text{Hz}$), causing less phase distortion and becomes more aggressive for higher frequencies. We also enclose the sensor board in Sensys' custom proprietary packaging and embed the sensor inside the pavement, thus attenuating any sound before it reaches the accelerometer. We tested the response of the sensor to loud sounds both in lab and in the field; it was very unresponsive to any sound.

3.1.3 Casing: Sound isolation and in-pavement installation

The circuit board and the battery are placed into the hard plastic casing as shown in Figure 2. The casing is then filled with fused silica and sealed air tight. This protects the electronics from rain water, oil spills etc on the road and helps in attenuating interference due to sound.

3.1.4 Circuit Description

Figure 3 shows the block diagram of the electronic circuit. The accelerometer and the operational amplifiers are powered by a 2.5 V supply voltage that can be turned on/off by the microcontroller as needed. The amplifier stage of the circuit subtracts a DC offset voltage from the accelerometer output and amplifies this difference by a gain of 10. This offset voltage is chosen to center the output of this stage at 1.25 V when there are no vibrations in the vicinity. The gain of 10 reduces the range of the accelerometer to $\approx \pm 225$ mg. This was necessary in order to ensure that the quantization noise from the analog-to-digital converter (ADC) is less than the noise from the accelerometer, otherwise the

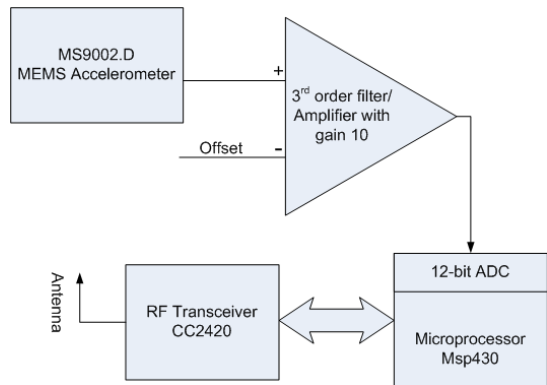


Figure 3: Block Diagram of the vibration Sensor.

resolution of the system would be limited by ADC noise. The reduced range is still sufficient as the expected acceleration range even for the heavy trucks is $\pm 200\text{mg}$ [1, 21]. The output of the amplifier stage is then sampled by the 12-bit ADC, and the collected samples are transmitted via the radio transceiver.

3.2 Communication Protocol Design

For wireless communication, we adapted the Synchronous Nanopower Protocol (SNP) detailed in [11]. The architecture of the protocol consists of three logical entities: an Access Point (AP), an optional repeater, and wireless sensor nodes. The protocol ensures clock synchronization of all nodes within 60 μs while minimizing the power consumption of nodes.

3.2.1 PHY Layer

The AP and all the nodes use IEEE 802.15.4 compatible radio transceivers. The transceiver uses the 2.4 GHz ISM band at a data transmission rate of 250 kbits/s and can be operated on one of 16 IEEE 802.15.4 compliant RF channels. The AP has a wired connection and a wireless connection, while the sensor nodes only have a wireless connection. The wireless connection is used to communicate with the sensor nodes while the wired connection of the AP is used to communicate with a computer running the Sensys' graphical user interface used to issue commands to the AP and the sensor nodes.

3.2.2 MAC Layer

The MAC layer is TDMA based and uses headers very similar to IEEE 802.15.4 MAC layer. Time is divided into multiple frames with each frame about 125 ms long. Each frame is further divided into 64 time slots, numbered 0 to 63, most of which can be used by the sensor nodes to transmit data. Timeslot 0 is used by the AP to send clock synchronization information and other commands to the sensors. The AP assigns every node unique time slots and a network address (or node ID) to communicate with it. This schedule enables individual nodes to stay awake for the minimum amount of time and prevents any packet collisions in the network.

3.2.3 Application Layer

There are three main applications that are used in the

protocol:

I. Sync Application: The basic TDMA structure is defined by this application. Sync packets are sent by the AP on a periodic basis with very low jitter. Nodes must first synchronize their clocks to these sync packets before they are allowed to transmit. When a sensor node first starts, it listens to sync packets every 125 ms. It learns the difference between its clock and the AP's clock, and over time improves its estimate of the AP's clock. As the estimate improves, the node converges to steady state in which it listens for a sync packet only once in 30 s. If a node loses sync, it repeats the above process to get synchronized again. In addition to sending clock information, the sync application is also used to send commands to individual sensors. Some of the useful commands sent are:

- *Set Mode:* used to switch between the Idle mode and Raw Data mode in Accelerometer application.
- *Reset:* used to reset the node to factory defaults.
- *Set Timeslot:* used to set the timeslot of the sensor.
- *Set RF Channel:* used to set the RF channel of the sensor.
- *Download Firmware:* used to put the sensor node in over-the-air software programming mode.
- *Set ID:* used to change the sensor node ID.

The node's clock is synchronized to within $\pm 60 \mu\text{s}$ of the AP's clock under this protocol. The sync application is always running in the background and other applications can run concurrently with it.

II. Accelerometer Application: The accelerometer application is the most important application for the vibration sensor. The application controls when to turn on the accelerometer and related circuitry, when to sample, and when to wake up the radio to transmit the vibration data collected.

- *Idle Mode (Mode E):* This is the default power saving mode of each sensor node. In this mode, the accelerometer and related conditioning circuitry are turned off by disabling the voltage regulator that powers this part of the circuit. Even the microcontroller and the radio transceiver are put to a low power consuming state for the majority of time. Once every 30 seconds, the microcontroller and the transceiver wake up and acquire the sync packet.
- *Raw Data Mode (Mode AccelR):* In this mode the accelerometer and related circuitry are turned on. The microcontroller wakes up every $1/512$ seconds and samples the analog output from the accelerometer unit, as shown in Figure 3. In addition to waking up for the sync packet, the transceiver wakes up right before its allotted timeslots to send the sampled data. We collect 32 samples at a sampling frequency of 512 Hz, each sample containing 12 bits of information. Thus, in every frame (125 ms) we accumulate 96 bytes of useful information to transmit. In order to have a reasonable packet size, we fragment the data in two parts, 48 bytes each, and transmit it using two different time slots 62.5 ms apart. The AP receives data from each sensor, appends useful information such as the time stamp, Received Signal Strength Indicator (RSSI), the Link Quality Indicator (LQI), and records it into a file that can be processed as desired.

III. Download Firmware Application: For maximum flexibility, the protocol allows a user to reprogram the entire flash memory of a sensor node over the air, via an AP. The general procedure for downloading new code consists of having the AP transmit new code repeatedly and the node updating its code in small pieces. In order to aid the management of code in the flash memory, each program is appended with a program header, which contains a description of the program, its address and length, its interrupt vectors, and some other information. The download stream actually contains two copies of the download code linked at different addresses. Only the data in addresses that do not overwrite the current running program are updated by the node. An algorithm is used to decide, based on all stored program headers, which program to run after download. The algorithm picks the highest priority image most recently downloaded, reboots and starts with this program.

The vehicle detection sensor follows the same protocol with a few minor differences. The required sampling for this application is just 128 Hz. For our purposes, we only use one of the modes of this sensor in which it transmits a vehicles arrival and departure times. Since there isn't a continuous stream of data to transmit in this mode, every packet is retransmitted until an acknowledgement is received from the AP.

3.3 Sensor Calibration Procedure

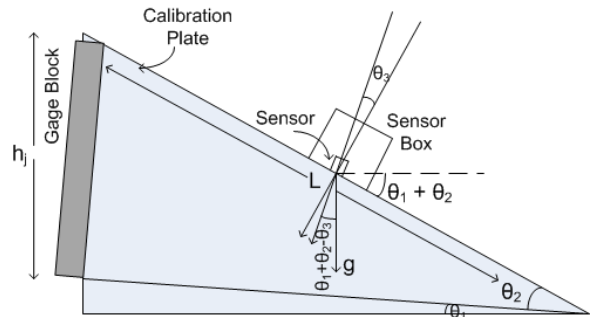


Figure 4: Calibration Setup

This section describes the procedure we use to calibrate the sensors for their sensitivity (V/g) and resolution (μg). Figure 4 models the calibration setup used. The idea is to use gage blocks of different heights to change the inclination of the sensor box, thus changing the component of acceleration due to gravity (g) along the sensing direction of the accelerometer. We estimate the sensitivity (V/g) of the accelerometer by using the sensor output at different acceleration levels. Using simple geometry, the component along the sensing axis of the accelerometer is $g \cos(\theta_1 + \theta_2 - \theta_3)$. If we let α be the sensitivity, $\theta = \theta_3 - \theta_1$ be the net tilt, h be the height of gage block, L be the length of calibration plate, $A = ag \cos \theta$, $B = ag \sin \theta$, then the output voltage (v)

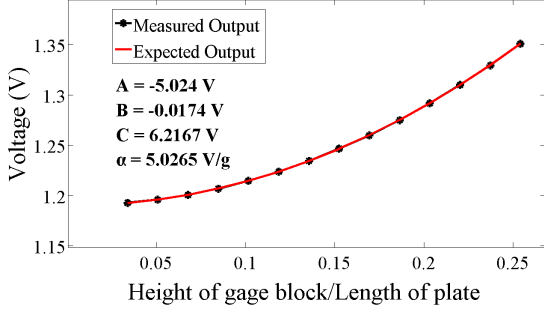


Figure 5: Calibration results for sensitivity. The expected output is the regression line.

must be:

$$\begin{aligned}
 v &= \alpha g \cos(\theta_2 - \theta) \\
 &= \alpha g \cos \theta_2 \cos \theta + \alpha g \sin \theta_2 \sin \theta \\
 &= A \cos \theta_2 + B \sin \theta_2 \\
 &= A \sqrt{1 - \left(\frac{h}{L}\right)^2} + B \left(\frac{h}{L}\right) \\
 &= A \sqrt{1 - x^2} + Bx. \tag{1} \\
 \alpha &= \sqrt{A^2 + B^2}. \tag{2}
 \end{aligned}$$

In reality, the measured output at a given inclination is never constant and fluctuates around some mean value due to noise in the surroundings and electronics. We model this by adding a zero mean gaussian random variable to equation (1). To estimate A, B and the sensitivity (α), given by equation (2), we measured the sensor output at different inclinations. At every inclination we collected 2500 samples (sampling frequency: 512 Hz) of data. We used linear regression to estimate the A and B in equation (1). Figure 5 shows the calibration results and the estimated sensitivity of one of the sensors. To estimate the resolution of the sensor we divide the standard deviation of the collected data by the estimated sensitivity. This gives us a measure of noise in the recorded acceleration. For this particular sensor, the resolution was found to be $388 \mu\text{g}$. All the other sensors had similar calibration results.

3.4 Sensor Performance Benchmarks

3.4.1 ADC performance

As we discussed earlier, we amplify the signal from the accelerometer to ensure that the quantization noise from the 12-bit ADC is not the limiting factor for the resolution of the system. To verify the acceleration reported by the vibration sensor, we compare its reported measurements with the output of the amplifier stage (Figure 3) measured by a 24-bit data acquisition system (DAQ) from National Instruments. The vibrations were generated by applying an impulse like input (using a hammer) to the surface the sensor sat on. Figure 6 shows that the two data sets are in very close agreement. The Fast Fourier Transform of the signal, in Figure 7, shows there is almost no energy in the signal around 256 Hz, confirming there is no significant aliasing during sampling. The sampling frequency of the sensors was verified by measuring it using an oscilloscope and was

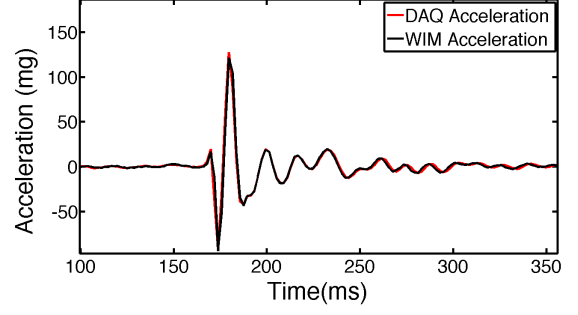


Figure 6: Comparison of data collected by the vibration sensor and a 24-bit DAQ.

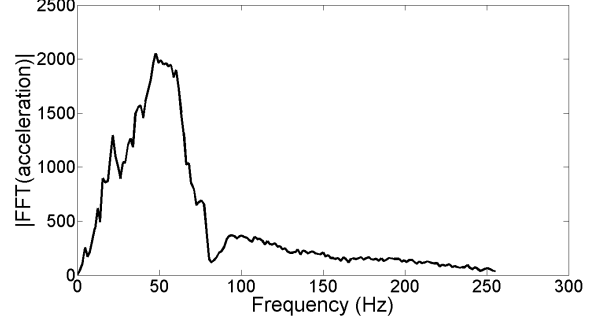


Figure 7: Fast Fourier Transform of the data measure by vibration sensor.

found to be $512 \pm 0.2 \text{ Hz}$.

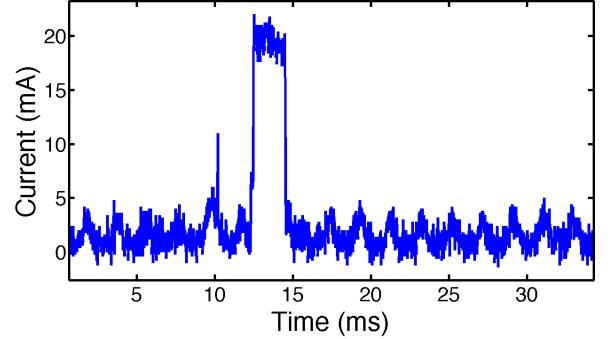


Figure 8: Current consumption in Raw Data mode.

3.4.2 Current Consumption

The average current consumption of the vibration sensor in both modes was estimated by connecting a resistor in series to the circuit board, measuring the voltage across it and using ohm's law to calculate the current drawn from the battery.

Mode AccelR. Figure 8 shows the current consumption in one of the transmit cycles. The square pulse in the plot is when the radio is turned on and actively transmitting. As expected, sending a packet over the radio consumes most of the current, but since we only transmit for about 2ms in 62.5ms, the duty cycle is relatively low and thus the average

current consumption is much lower and found to be 1.96 mA. It is interesting to note that the transmission of a packet of 48 bytes takes about 2ms (estimated from the width of the pulse), which almost occupies two time slots. The oscillations seen in the baseline of this plot are due to the extra current consumption, every 1.95 ms (512 Hz), when the 12-bit ADC samples. The current consumption by the ADC can be reduced by using the external source of voltage reference instead of the internal 2.5V reference. This, however, reduces the effective number of bits (ENOB) of the ADC.

Mode E. In the idle mode, most of the circuitry is turned off or in sleep mode, except when a sync packet is acquired. The duty cycle for this (once in 30 s) is very low and so is the average current consumption. Average current consumption in this mode was found to be 35 μ A.

Expected Lifetime. Using a 7200 mAh battery, the sensor can last over 23 years in Mode E and over 5 months in Mode AccelR. If needed, the lifetime in the raw data mode can be increased by compressing the data. This, however, won't be necessary once we implement the axle detection algorithm in the sensor. The only data that needs to be transmitted in that case are the axle count and the axle separation in time. This reduction in amount of data that needs to be transmitted would increase the lifetime in this mode to several years.

4. AXLE DETECTION ALGORITHM

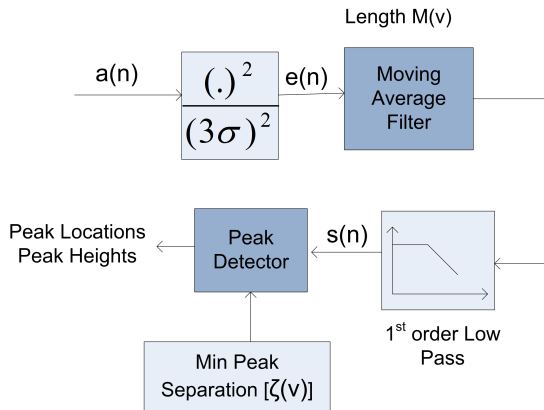


Figure 9: System representation of the Axle Detection Algorithm. The moving average filter length (M) and the minimum peak separation (ζ) depend on the velocity of the vehicle.

4.1 ADET Algorithm Description

Each moving axle can be modeled as a moving impulsive force applied on the pavement. This force causes the pavement and sensors to vibrate such that the measured acceleration decays in time. The overall acceleration measured for a multi-axle vehicle, as shown in Figure 11, has this signature decaying waveform due to each axle. It is very easy to spot the different axles from the measured acceleration if the signal due to each axle is sufficiently separated in time, i.e. the effect of the past axles has sufficiently decayed before the arrival of a new axle. This is often not the case at highway speeds.

Instead we need to rely on a statistical approach to axle detection. The running average of the energy of an axle with an appropriately chosen time window can still manifest appropriate separation even with moderate overlaps in the acceleration signal. We propose an algorithm ADET for axle detection based on this idea.

Figure 9 shows the block diagram of ADET. It finds the smooth energy envelope of measured acceleration, and locates the peaks that are sufficiently separated in time. The signal $a(n)$ is first divided by 3 times the noise (found in Section 3.3). This ensures that in the absence of an axle the signal is below 1. The normalized signal is then squared to calculate the energy. This step further increases the signal to noise ratio (SNR) as noise is attenuated by squaring whereas the signal, which is greater than 1, is amplified.

The next step is smoothing of $e(n)$ by passing it through a moving average filter (MAF) with $M(v)$ taps to obtain its envelope. The number of taps determines the bandwidth of the filter. Since the bandwidth of the measured acceleration signal increases linearly with the speed of the vehicle [2], the cut-off frequency of the filter needs to be speed dependent as well. Using data from four trucks at different speeds, we observed the bandwidth of the energy signal and empirically defined $M(v) = \frac{900}{v}$. An additional stage of a single pole low pass filter with a fixed cutoff is used to further smoothen the signal. This step is optional and in practice we observed that similar results are obtained even in its absence.

The last step finds peaks in the smooth energy ($s(n)$) with a minimum time separation ($\zeta(v)$). This step ensures that local variations around peaks of $s(n)$ are not detected as new axles. Minimum time separation for axles was chosen by assuming that the axles are at least 6 ft apart. Weigh stations typically consider tandem axles as one axle and therefore ground truth data also counted tandem axles as one axle. Tandem axles are typically between 4 and 5 ft apart. It is important to note that by reducing the minimum axle separation to less than 4 ft, the algorithm is able to detect both the axles in the tandem axle but for the sake of easy comparison with the collected ground truth data we kept it at 6 ft. Converting the axle separation to time separation we obtain $\zeta(v) = \frac{6}{v}$.

A heuristic mathematical analysis of the procedure is shown in Appendix A which confirms the choices for the filter length and power of the procedure.

4.2 Wide Lane ADET: Combining Multiple Sensors

When the lane is wide vehicles can experience significant wander movement inside the lane. For example, substantial wander is observed at the wide approaches that connect the exits of truck inspection stations to the highway. Trucks are moving from right to left in the approach as they get ready to merge into the highway.

In such situations a single vibration sensor at the center of the lane fails to capture the vehicle in its entirety. If ADET is applied to the single sensor, most likely the number of axles will be undercounted. Instead we propose a modification of our system that combines vibration readings from multiple sensors.

If a truck wanders across a lane, and a vibration sensor array covers the width of the lane it is expected that at least one sensor will measure the strongest vibration signal. This is the idea behind the wide lane extension of ADET. It uses

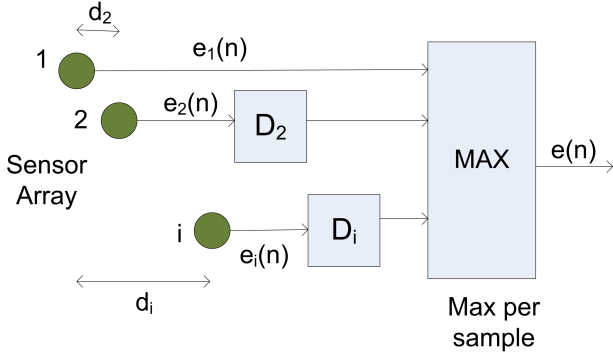


Figure 10: System representation of the adjustment made to correct vehicle wander.

a redefinition of the notion of energy ($e(n)$) in Figure 9 as $e(n)$ in Figure 10. The energy of the total signal at time n is the maximum of the energy of the individual signals $e_i(n)$ of each sensor i .

Since the sensors are spatially offset in their installation, the peak energy due to a single axle is measured by the sensors at different times. For instance sensor 2 will measure the peak energy a little later than sensor 1. Therefore, the individual energy measurements need to be appropriately *delayed*. The delay D_i for each sensor i can be easily computed given the speed v of the vehicle and the distance d_i between sensor i and sensor 1 in the installation: $D_i = d_i/v$. Now instead of using a single sensor, perhaps the one with maximum total energy, we choose maximum instant energy from each sensor to make a new time series. The $e(n)$ produced here can be processed using ADET as before.

4.3 Estimating Axle Spacing

ADET also outputs for each axle k the time of peak detection t_k . Using the speed v of the vehicle, the axle spacing s_k between axles k and $k+1$ can be determined using

$$s_k = v(t_{k+1} - t_k).$$

Notice that in a non-wide lane scenario with multiple sensors installed, there is no significant wander and therefore the spacing estimates can be done using a single sensor and then averaged to obtain a global, more accurate estimate.

4.4 Application of ADET

To illustrate the algorithm, we show the results of applying ADET to data measured from a single vibration sensor, and for a truck (Truck 49) of the class shown in Figure 12. The setup used to acquire the data is explained in Section 5 and shown in Figure 13. The data was acquired from sensor L.

Data Cleansing. Before applying ADET to the vibration data, we remove the mean of the measured acceleration. This removes any transient effects of filtering the data. For occasional packet drops (even with the retransmission), we replace the unknown data by the last received data value.

Results for Truck 49. Figure 11 shows the results when ADET is applied to truck number 49 in the dataset. The improvement in the SNR can be seen by comparing the peaks to the baseline (or noise) for $a(n)$ and $e(n)$. The envelope of $e(n)$ or the smooth energy is shown as $s(n)$. The peaks of $s(n)$ signify the individual axles. The axles detected by

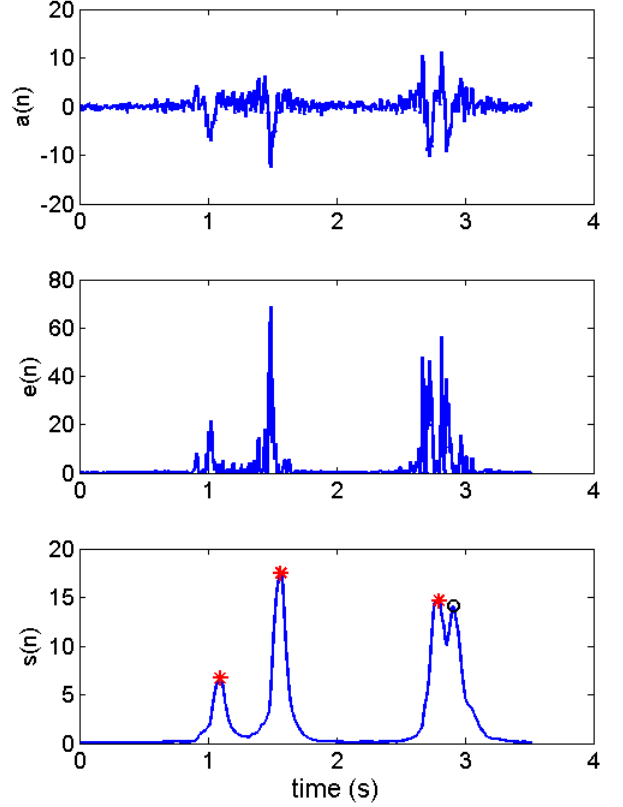


Figure 11: Results of ADET on truck 49 (two single axles and one tandem axle), $a(n)$ is the measured acceleration in mg, $e(n)$ is the scaled energy in mg^2 , and $s(n)$ is the smooth energy in mg^2 . The red asterisks on $s(n)$ are the axle locations found by ADET. By reducing the minimum axle separation, the individual axles in the tandem axle can also be detected, as shown by the black circle.

ADET are shown as red asterisks on $s(n)$. Note that ADET only detected one of the last two peaks in $s(n)$, thus counting the tandem axle as only one axle. By reducing the minimum axle separation to 3 ft, ADET successfully detects both axles in the tandem axles as shown by the black circle.

5. DEPLOYMENT ON HIGHWAY I-680

5.1 Experimental Setup

With the permission of California Highway Patrol, 4 vibration sensors and 4 vehicle detection sensors were installed on California Highway I-680 as shown in Figure 13. The site is a highway on-ramp used by vehicles coming from the Sunol Weigh Station. The site was particularly suitable since the vehicles slowed down at the weigh station and gave us enough time for collecting ground truth data on the number of axles. Two researchers collected data: Researcher 1 at the weigh station and Researcher 2 on the side of the highway near the AP. Researcher 1 noted the vehicle



Figure 13: Top left shows a truck approaching the sensors and not traveling in a straight line. Top right shows the sensors embedded in the pavement. Bottom shows the WSN setup at Sunol site. D, H, M, N are vehicle detection sensors whereas I, J, K, L are vibration sensors. Dimensions are in inches unless specified otherwise.



Figure 12: Picture of a FHWA class 7 (2S2) truck.

description, its number of axles, and signalled Researcher 2 via a cellular phone about the upcoming test vehicle. Researcher 2 triggered the AP to start logging the data from all sensors at the arrival of test vehicle and noted the vehicle description for comparison. Data from 53 different trucks, ranging from pickup trucks to 5-axle commercial trucks, was collected.

5.2 Installation Procedure



Figure 14: Installation procedure for embedding the sensors in the pavement.

As shown in Figure 14 installing the sensors in the ground

involves boring a 4-inch diameter hole approximately $2\frac{1}{4}$ inches deep at the desired location, placing the sensor into the hole so that it is properly leveled with the earth's surface, and sealing the hole with fast-drying epoxy [23].

5.3 Deployment Challenges

Packet Drops. While testing in the lab, we were able to receive data from the sensor at 50 feet away, and in the presence of other wireless equipment like cell phones, bluetooth devices and WiFi devices. However, we dropped quite a few packets while testing in the field. Even though the packet drop rate was low (1 %), the packets were dropped when the vehicle was on top of the sensors causing the loss of useful information. To fix this problem, we tried simple retransmission of the packets with a delay of 1 packet i.e. we send the current packet (packet 1), the next packet (packet 2), packet 1 again, and then packet 2 again. By interleaving the packets in this way, we could drop up to two consecutive packets and still not lose any information. After implementing retransmissions we reduced the useful information drop rate to almost zero.

Vehicle Wander. Since the sensors were installed on a highway on-ramp and vehicles were in the process of merging on to I-680 when they went over the sensors, very often they were not traveling straight in the lane as shown in Figure 13. Ideally, we would like choose the data from the vibration sensor that was closest to the vehicle's tires because it will have the maximum vibration signal but due to wandering different axles/tires of the same vehicle were closer to different sensors. The solution of this problem is

to use Wide Lane ADET algorithm in Section 4.2 .

Sensor Failure. Sensor K, as seen in Figure 13, did not work after installation and is being recovered for inspection. Thus, vibration data was available only from 3 sensors.

6. EXPERIMENTAL RESULTS

In this section we evaluate the performance of the proposed WSN system and ADET in the data collected at the I-680 site. For the experiments we used sensors H and M (see Figure 13) for speed estimation. Section 6.2 discusses the noise of the vibration sensor measured in the field, Section 6.2 the performance of ADET and Wide Lane ADET and Section 6.3 concludes with an analysis of axle spacing estimates.

6.1 Vibration Sensor Performance

We measured the noise of the installed vibration sensor with no vehicle in vicinity and found it to be $414 \mu\text{g}$ RMS. When we compared this to all the truck data we collected, we found that the acceleration amplitude in all trucks was greater than 10 mg and therefore significantly higher than the sensor noise. Most of the noise is due to ambient vibrations induced by the environment surrounding the road. The amplitude of the noise depends on the layered structure of the road. However, in practice we observed identical noise levels in a road made with different materials in different layers, but same layered structure.

We also measured the noise when a truck was parked on top of the sensors, truck engines were on in one case and truck blew its horn in another. Compared to vibrations due to a moving axle, there were no additional peaks in the measured. The noise level increased slightly for each case, and it was 7% and 4% higher respectively.

Using incoming acceleration data measured continuously for 2 hours on a real-time plot and paying special attention to when a heavy vehicle traveled in the closest lane, we evaluated the effect of vehicles in nearby lanes. The sensors did not register any noticeable peaks, whereas even the lightest pickup truck in the same lane as the sensors had appreciably high peaks. This supports the fast decay of the seismic waves [8] so vibrations from nearby lanes decay before reaching the sensor.

6.2 Axle Count

We applied ADET to each sensor individually and applied adjusted ADET to all sensors combined for all 53 trucks. Count error is defined to be the difference between the ground truth axle count and the estimated axle count. Table 2 summarizes the performance of the two algorithms. The maximum axle count error is 3, sensor I under-counts 3 axles of a truck in this case. By combining the measurements from all sensors, the algorithm always gives the correct axle count. Axle count performance is strongly affected by truck wander. Trucks that moved closer to the right side of the road caused errors in sensor I counting. Undercounting was observed because the signal becomes weaker as the tire is further from the sensor and thus noise affects peak detection performance. Similarly, sensors J and L experience undercount errors when the truck moves diagonally from right to left due to the geometry of the merge at the site. Some axles are captured but not others. Since wander is always present in actual lanes, multiple sensors will be required in counting deployments.

Count Error	Sensor I	Sensor J	Sensor L	Combined
3	1	0	0	0
2	1	2	1	0
1	2	2	3	0
-1	3	1	1	0
Correct	46	48	48	53
Performance	86.8%	90.6%	90.6%	100%

Table 2: Performance of ADET using individual sensors and combination of sensors. Count Err. is the difference between the ground truth and ADET estimate. Under each sensor column is the observed frequency of the errors

6.3 Axle Spacing

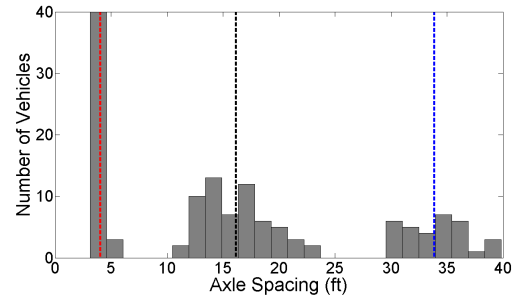


Figure 15: Distribution of estimated axle spacings. There are three clusters in the data separated by empty bins. The dotted lines represent the means of these clusters.

We estimate the axle spacings using multi-sensor ADET. Figure 15 shows the distribution of estimated axle spacings. The data appears to be naturally clustered into three different groups separated by empty bins in the histogram. The first cluster includes axles that are spaced between 3 ft and 6 ft. This is very typical for tandem axles and provides encouraging evidence supporting the accuracy of the estimates. The second cluster is mostly accounted by pickup trucks, small two axle commercial trucks, and the first two axles of the larger commercial trucks. The third group is mostly comprised of axles of the trailers. A typical grandfathered Semitrailer in California [9] ranges between 48 ft to 53 ft and therefore axles spacings can be as large as 40 ft. The large variation in the second and third cluster in Figure 15 is expected and is consistent with Federal Highway Administration’s data [9].

Trucks at the weigh station could not be stopped for axle spacing measurement and therefore the only ground truth data we have for this section is the vehicle description. We compared the estimated axle spacings to the expected spacings based on the vehicle description and verified that the estimates were reasonable. One instance of such comparison involved two similar looking pickup trucks (numbers 14 and 46) and we found their estimated axle spacings to be 13.7 ft and 13.4 ft. We measured the axle spacing for a similar truck and found it to be 13.5 ft.

7. CONCLUSIONS AND FUTURE WORK

Conclusions. A wireless sensor network capable of vehicle classification based on axle count and spacing was suc-

cessfully implemented and tested. The requirements for using pavement vibrations to detect axles were identified. The pavement accelerations varied from 10 mg to 180 mg depending on the axle load. Range of ± 225 mg and bandwidth of 50 Hz is sufficient to capture the individual effect of axles on the pavement. Embedding the sensor in the pavement and the use of an aggressive low-pass filter isolates the sensor from vibrations due to sound. The sensor must be strongly coupled to pavement in order to measure the pavement acceleration accurately and the suggested installation procedure gets the job done.

The solution provided in this paper for vehicle classification has many advantages over existing technologies:

- Majority of the existing technologies are wired solutions instead of wireless.
- Both the sensors and the AP can be powered by batteries and consume much less power than other technologies.
- The installation procedure and the sensors themselves are much cheaper compared to others.
- There is minimal maintenance required whereas maintenance costs are a bulk of the total costs associated with some of the other technologies.

The wireless sensor network was deployed on I-680 and data was successfully collected. A novel algorithm that estimates the axle count and spacing from pavement acceleration was designed and tested on the collected data. The Axle Detection algorithm (ADET) is a combination of energy envelope detection and peak detection, and could be useful in many other applications. ADET is simple enough to be implemented on a sensor node with very limited processing power. A configuration of vibration sensors and vehicle detection sensors that can be used for axle detection was successfully tested. ADET was used on the data collected using this configuration for 53 different trucks. The estimated axle count was compared with the ground truth classification data with an accuracy of 100 percent.

Future Work. The main challenges for future deployments are: to find an optimal arrangement of sensors in order to minimize the number of sensors deployed; to reduce the amount of data transmitted while minimizing the packet drop rate; and to reduce the sensor power consumption. Optimized sensor arrangements can capture different cases of wander while minimizing the number of sensors needed. In its current form, ADET requires the full acceleration signal be transmitted to the base station for detecting axles but use of Discrete Cosine Transform (DCT) or wavelet approximation schemes could potentially reduce the amount of data transmitted, and still enjoy the benefits of combined ADET. It is also important to explore packet encoding or delaying schemes to reduce the packet drop rate further. Moreover, developing and deploying a distributed version of ADET and incorporating known axle length distributions into estimation are avenues of future work. Power consumption can be reduced drastically by implementing ADET inside the sensor but techniques to estimate the required velocity-dependent bandwidth of the smoothing filter need to be explored further. The sensing setup could also benefit from energy harvesting since truck loads cause substantial vibrations. The current setup also enables other interesting applications and

we are actively looking into truck load inference and pavement condition management schemes.

8. ACKNOWLEDGEMENTS

We would like to thank California Highway Patrol for allowing us to install sensors at the weigh station and use their office to collect ground truth data. Special thanks to Sebastian Lodahl for his help with the sensor installation, and David Baca for data collection. Many thanks to Christopher Flores for his help in finding vehicle classification standards. This project was funded by the National Science Foundation under Award Number IIP-0945919.

9. REFERENCES

- [1] R. Bajwa. Weigh-in-motion system using a mems accelerometer. Technical report, EECS Department, University of California, Berkeley, 2009.
- [2] D. Cebon. *Handbook of Vehicle-Road Interaction*. Swets and Zeitlinger Publishers, 1999.
- [3] M. Ceriotti, L. Mottola, G. Picco, A. Murphy, S. Guna, M. Corra, M. Pozzi, D. Zonta, and P. Zanon. Monitoring heritage buildings with wireless sensor networks: The Torre Aquila deployment. In *Information Processing in Sensor Networks, 2009. IPSN 2009. International Conference on*, pages 277–288. IEEE, 2009.
- [4] S. Y. Cheung, S. Coleri, B. Dundar, S. Ganesh, C.-W. Tan, and P. Varaiya. Traffic measurement and vehicle classification with single magnetic sensor. *Transportation Research Record: Journal of the Transportation Research Board*, 1917:173–181, 2006.
- [5] Colibrys, Inc, accelero.us@colibrys.com. *MEMS Capacitive Accelerometers Datasheet MS9000.D*.
- [6] M. Duarte and Y. Hen Hu. Vehicle classification in distributed sensor networks. *Journal of Parallel and Distributed Computing*, 64(7):826–838, 2004.
- [7] Federal Highway Administration, U.S. Department of Transportation. *Traffic Monitoring Guide*, May 2001.
- [8] M. C. Fehler. *Seismic Wave Propagation and Scattering in the Heterogeneous Earth*. Springer, 2009.
- [9] http://ops.fhwa.dot.gov/freight/publications/size_regs_final_rpt/index.htm#length, 2009.
- [10] S. Gupte, O. Masoud, R. Martin, and N. Papanikolopoulos. Detection and classification of vehicles. *Intelligent Transportation Systems, IEEE Transactions on*, 3(1):37–47, 2002.
- [11] A. Haoui, R. Kavaler, and P. Varaiya. Wireless magnetic sensors for traffic surveillance. *Transportation Research C*, 16(3):294–306, 2008.
- [12] C. Harlow and S. Peng. Automatic vehicle classification system with range sensors. *Transportation Research Part C: Emerging Technologies*, 9(4):231 – 247, 2001.
- [13] R. I. S. John H. Wyman, Gary A. Braley. Evaluation of fhwa vehicle classification categories. Technical report, Federal Highway Administration, 1984.
- [14] S. Kim, S. Pakzad, D. Culler, J. Demmel, G. Fennes, S. Glaser, and M. Turon. Health monitoring of civil infrastructures using wireless sensor networks. In *IPSN '07: Proceedings of the 6th international conference on Information processing in sensor networks*, pages 254–263, New York, NY, USA, 2007. ACM.

- [15] A. N. Knaian. A wireless sensor network for smart roadbeds and intelligent transportation systems. Master's thesis, Massachusetts Institute of Technology, 2000.
- [16] M. Li and Y. Liu. Underground structure monitoring with wireless sensor networks. In *Proceedings of the 6th international conference on Information processing in sensor networks*, pages 69–78. ACM, 2007.
- [17] C. Merzbacher, A. Kersey, and E. Friebele. Fiber optic sensors in concrete structures: a review. *Smart materials and structures*, 5:196, 1996.
- [18] L. E. Y. Mimbela and L. A. Klein. A summary of vehicle detection and surveillance technologies used in intelligent transportation systems. Technical report, New Mexico State University, 2000.
- [19] A. Nooralahiyan, M. Dougherty, D. McKeown, and H. Kirby. A field trial of acoustic signature analysis for vehicle classification. *Transportation Research Part C: Emerging Technologies*, 5(3-4):165–177, 1997.
- [20] A. V. . Oppenheim, R. W. Schaffer, and J. R. Buck. *Discrete-Time Signal Processing*. Prentice-Hall, 2nd edition, 1999.
- [21] R. Rajagopal. *Large Monitoring Systems: Data Analysis, Deployment and Design*. PhD thesis, University of California, Berkeley, 2009.
- [22] H. Sawant, J. Tan, and Q. Yang. A sensor networked approach for intelligent transportation systems. In *Intelligent Robots and Systems, 2004. (IROS 2004). Proceedings. 2004 IEEE/RSJ International Conference on*, volume 2, pages 1796 – 1801 vol.2, 2004.
- [23] Sensys Networks, Inc, 2650 9th Street, Berkeley CA 94710. *The Sensys Wireless™ Vehicle Detection System*, 1.1 edition.
- [24] Silicon Designs, Inc. *Model 1221 Low Noise Analog Accelerometer*.
- [25] C. Sun and S. Ritchie. Heuristic vehicle classification using inductive signatures on freeways. *Transportation Research Record: Journal of the Transportation Research Board*, 1717(-1):130–136, 2000.
- [26] N. Xu, S. Rangwala, K. K. Chintalapudi, D. Ganesan, A. Broad, R. Govindan, and D. Estrin. A wireless sensor network for structural monitoring. In *SensSys '04: Proceedings of the 2nd international conference on Embedded networked sensor systems*, pages 13–24, New York, NY, USA, 2004. ACM.

APPENDIX

A. MODEL ANALYSIS OF ADET

A.1 Model of a Single Axle

In [21] (Chapter 7, Theorem 1) it is shown that the displacement response at location x and time t to a moving axle with speed V in a smooth road can be approximated by

$$y(x, t) = F \times \Phi(Vt - x), \quad (3)$$

where F is proportional to the axle weight and $\Phi(r)$ is a function defined for both $r \geq 0$ and $r < 0$. It also has the property that its maximum is $|\Phi(0)|$ and goes to zero exponentially with $r \rightarrow \pm\infty$. Notice this property implies that the signal $y(x, t)$ is maximum at $t = x/V$, i.e., when the axle is at the location where the sensor is.

A.2 ADET applied to a measured signal

We approximate the behavior of ADET in the measured signal by following a continuous time analysis. This gives a heuristic understanding of the procedure, but also can be used with technical modifications to show properties for a sampled system. First notice that for a fixed location, the acceleration is given by $\ddot{y}(x, t) = FV^2 \times \ddot{\Phi}(Vt - x)$. Since the measurement is noisy, assume that a sensor measures $z(t) = \ddot{y}(x, t) + \eta(t)$, where $\eta(t)$ is a white noise with variance σ^2 . Now, the output of the mean filter of length τ/V at time t :

$$\begin{aligned} z(t) &= \frac{1}{\tau/V} \int_t^{t+\tau/V} [FV^2 \times \ddot{\Phi}(V\tilde{t} - x) + \eta(\tilde{t})]^2 d\tilde{t}, \\ &= \frac{1}{\tau} \int_{Vt-x}^{Vt-x+\tau} [FV^2 \times \ddot{\Phi}(r) + \eta(r/V + x/V)]^2 dr, \\ &= \frac{1}{\tau} \int_{Vt-x}^{Vt-x+\tau} \{V^4 [F \times \ddot{\Phi}(r)]^2 dr \\ &\quad + 2[FV^2 \times \ddot{\Phi}(r)\eta(r/V + x/V)]dr \\ &\quad + \eta(r/V + x/V)^2 dr\} \\ &= V^4 z_0(Vt - x) + \frac{1}{\tau} \int_{Vt-x}^{Vt-x+\tau} \eta(r/V + x/V)^2 dr \\ &\quad + V^2 \frac{2F}{\tau} \int_{Vt-x}^{Vt-x+\tau} \ddot{\Phi}(r)\eta(r/V + x/V)dr \\ &\approx V^4 z_0(Vt - x) + \frac{\sigma^2}{\tau/V} \int_0^{\tau/V} \eta(\tilde{t})^2 / \sigma^2 d\tilde{t}. \end{aligned}$$

The approximation in the last equation is due to assuming the fluctuations in the next to last term is a zero mean term with bounded variance proportional to V^4/τ^2 , so for large enough windows, it can be assumed zero. The white property of the random process is used as well. The expectation of the second term is σ^2 . More importantly, the first term is the filtered term obtained for a unit speed example with magnitude proportional to V^4 . Furthermore, since

$$z_0(t) = \frac{1}{\tau} \int_t^{t+\tau} \ddot{\Phi}(r) dr,$$

the peak of $z_0(t)$ will coincide with the peak of $\ddot{\Phi}(r)$ if τ is sufficiently small. Thus the variable τ represents a choice of *peak width*. Finally, from the definition of Φ it is possible to show that the peak of $\ddot{\Phi}$ coincides with that of Φ in this problem. Thus we have justified that the *peak* of $z_0(t)$ is an axle and moreover the timing of the peak is the time when the axle is at the location where the sensor is installed.

A more careful analysis of the noise term can even reveal the error term for the peak location under the given noise assumptions. But a simple observation shows the power of the method. While the noise has variance $V^2/\tau^2\kappa$ where $\kappa = E[X^4]$ for X gaussian, the signal has power proportional to V^8 . Intuitively, for a false peak to overcome a true peak the noise would have to have a deviation of order $O(V^6)$.